DESIGN AND APPLICATION OF SQUEEZE FILM DAMPERS FOR TURBOMACHINERY STABILIZATION

by

Edgar J. Gunter, Jr.
Professor

L. E. Barrett
Research Engineer

P. E. Allaire
Assistant Professor

University of Virginia
Charlottesville, Virginia

Edgar J. Gunter received a B.S.M.E. degree in 1956 from Duke University, a M.S. degree in Engineering Mechanics in 1961 and a Ph.D. in Engineering Mechanics in 1965 from the University of Pennsylvania.

He was with Clark Brothers Company, Olean, New York from 1956-1959 and was with Franklin Institute, Philadelphia, Pennsylvania from 1962-1965.

Dr. Gunter is a member of several professional societies. He has over 50 publications, technical notes, and technical reports in the area of bearings and rotor dynamics.

L. E. Barrett holds a B.S. and an M.S. degree in Mechanical Engineering. He is a Rotor Dynamics Research Engineer at the University of Virginia. He has been actively involved with the analysis of squeeze film dampers for turbomachinery for the past three years for NASA and industry and has been involved in the design of squeeze film dampers for several industrial machine applications. He is also involved in the area of unbalance response and balancing of high speed flexible rotors.

Dr. Paul Allaire received his B.S. in Mechanical Engineering in 1963 and his M.S. degree from Yale in 1964, and the Ph.D. degree from Northwestern University in 1972.

He is co-director of the Rotor Dynamics Research Laboratory of the University of Virginia with Dr. Gunter and specializes in the application of finite element techniques to fluid mechanics problems. He is currently involved in the analysis of multilobed, tilting pad, and squeeze film damper bearings for turbomachinery.

ABSTRACT

This study investigates the steady-state and transient response of the squeeze film damper bearing. Both the steady-state and transient equations for the hydrodynamic bearing forces are derived. The steady-state equations are used to determine the damper equivalent stiffness and damping coefficients. These coefficients are used to find the damper configuration which will provide the optimum support characteristics based on a stability analysis of the rotor-bearing system. The effects of end seals and cavitated fluid film are included.

The transient analysis of rotor-bearing systems is performed by coupling the damping and rotor equations and integrating forward in time. The effects of unbalance, cavitation and retainer springs are included in the analysis.

Methods of determining the stability of a rotor-bearing system under the influence of aerodynamic forces and internal shaft friction are discussed. Particular emphasis is placed on solving the system characteristic frequency equation and stability maps produced using this method are presented.

The study shows that for optimum stability and low force transmissability the squeeze bearing should operate at an eccentricity ratio of $\epsilon<0.4$.

1. INTRODUCTION

Modern turbomachines are highly complex systems. Current design trends are producing machines that consist of several process stages joined together. The rotors in these machines are highly flexible shafts, often mounted in more than two bearings, that rotate at very high speeds. It is not uncommon to see machines that operate above the second critical speed. As a result the system dynamics are very complicated.

One of the major problems encountered in these machines is instability produced by aerodynamic forces on impeller wheels, friction in the stressed rotor and hydrodynamic forces in the bearings. The instability is characterized by large amplitude whirl orbits and often results in bearing or total machine failure. It is often aggravated by seals and other external forces transmitted to the machine. Production losses from failed machines are very high and it may take many months to repair or replace the failed unit. In addition operator safety is jeopardized when machines fail and occasional loss of life occurs.

NOMENCLATURE

SYMBOL		
C	Bearing clearance	in
C_o	Equivalent bearing damping	lb-sec/in
C_{xx}, C_{xy}	Bearing damping	lb-sec/in
C_{yy}, C_{yx}	Bearing damping	lb-sec/in
e	Journal eccentricity	in
EMU	Ratio of unbalance eccentricity to bearing clearance	----
F_x	Force component in x-direction	lbf
F_y	Force component in y-direction	lbf
F_r	Force component in radial direction	lbf
F_θ	Force component in tangential direction	lbf
FMAX	Maximum hydrodynamic force	lbf
FU	Force due to rotating unbalance	lbf
FURATIO	Ratio of FMAX to FU	----
h	Fluid film thickness	in
$\vec{i}, \vec{j}, \vec{k}$	Unit vectors in fixed coordinate system	----
k_o	Equivalent bearing stiffness	lb/in

SYMBOL	DESCRIPTION	UNITS
KR	Retainer spring stiffness	lb/in
k_{xx}, k_{xy}	Bearing stiffness	lb/in
k_{yy}, k_{yx}	Bearing stiffness	lb/in
L	Bearing length	in
N	Rotor speed	RPM
$\vec{n}_r, \vec{n}_\theta$	Unit vectors in rotating coordinate system	----
P	Pressure	lb/in^2
PMAX	Maximum hydrodynamic pressure	lb/in^2
Q	Aerodynamic cross coupling	lb/in
R	Bearing radius	in
t	Time	sec
W	Weight	lbf
x,y,z	Displacements	in
μ	Viscosity	$lb\text{-}sec/in^2$
θ, θ'	Angular measure	----
$\dot{\phi}$	Journal precession rate	sec^{-1}
ω	Angular velocity	sec^{-1}

An example of violent self-excited whirl motion in a turbo-rotor is Fig. 1.1 which represents a centrifugal compressor designed to operate at 52,000 RPM. At the design speed the compressor becomes highly unstable, the magnitude of the whirl motion being dependent upon the compressor speed and loading. The occurrence of this type of whirl motion has caused several catastrophic failures with this class of compressors.

From the earliest investigations of rotor instability, it has been known that the use of flexible, damped supports has an effect on instability and can eliminate it or alter the speed at which it occurs. Recent research has produced a large body of knowledge on the use of these supports and their effect on instability.

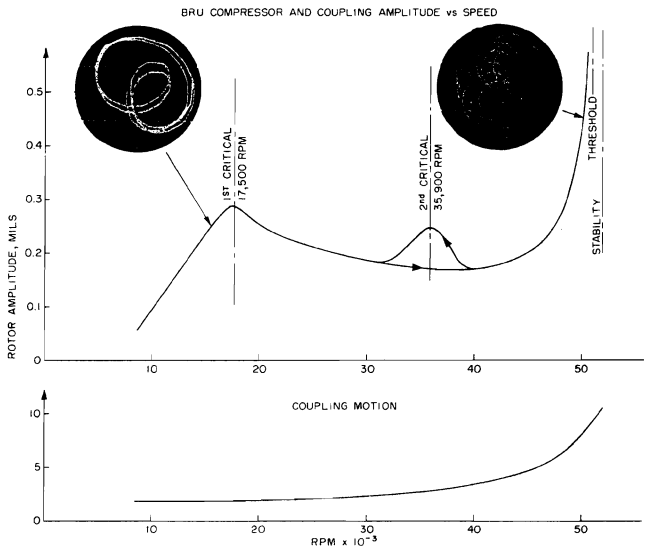

Figure 1-1. BRU Compressor and Coupling Amplitude vs Speed Showing Self-Excited Instability.

The squeeze film damper bearing as shown in Fig. 1-2 is one type of flexible support that is currently being investigated. This study examines the squeeze bearing and through computer simulation shows its effects on several rotor-bearing systems. The equations for the hydrodynamic damper forces are developed in both fixed and rotating coordinate systems. The use of two coordinate systems allows for both steady-state and transient analysis of damper performance.

The steady-state behavior of the damper results in the formulation of damper stiffness and damping coefficients which can be used to size the damper configuration. This is accomplished by comparing the coefficients with required values obtained from a stability analysis of the rotor-bearing system.

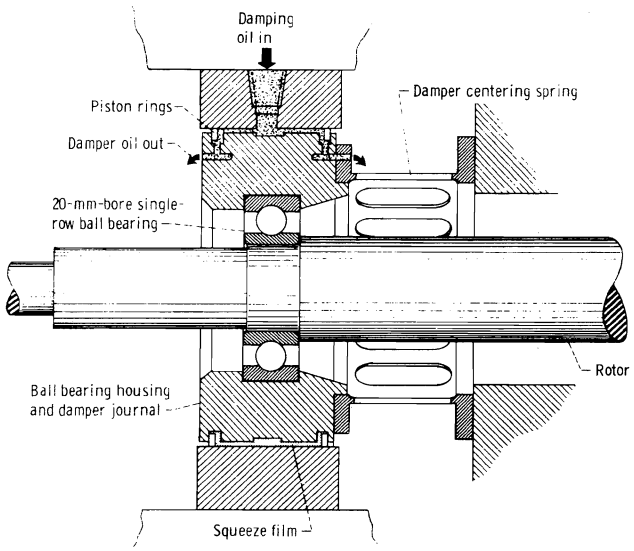

Figure 1-2. Squeeze-Film Damper with Central Feed Groove.

The transient analysis is very useful in determining the response to particular forms of external and internal forces as noted previously. Also the effect of damper retainer springs and fluid film cavitation can be found. The transient response is found by tracking the journal motion forward in time by integrating the equations of motion under the influence of the system forces.

2. THEORETICAL ANALYSIS

2.1 Reynolds Equation

The configuration of the squeeze film damper bearing is shown in Figure (2-1) where the clearance has been exaggerated. Both fixed and rotating coordinate systems are shown, and the bearing equations are derived for both systems. The definitions of the various parameters are listed in the nomenclature section of this paper.

The basic bearing equation is the Reynolds equation which is derived from the Navier-Stokes equations for incompressible flow. With the proper bearing parameters the equation for the fluid film forces are derived. [1]

The Reynolds equation for the short, plain journal bearing is given in both fixed and rotating coordinates by:

Fixed coordinates:

$$\frac{\partial}{\partial Z}\left[\frac{h^3}{6\mu}\frac{\partial P}{\partial Z}\right] = (\omega_b + \omega_j)\frac{\partial h}{\partial \theta} + 2\frac{\partial h}{\partial t} \qquad (2\text{-}1)$$

Rotating coordinates:

$$\frac{\partial}{\partial Z}\left[\frac{h^3}{6\mu}\frac{\partial P}{\partial Z}\right] = (\omega_b + \omega_j - 2\dot{\phi})\frac{\partial h}{\partial \theta'} + 2\frac{\partial h}{\partial t} \qquad (2\text{-}2)$$

As shown in Figure (2-1), the angle θ in the fixed coordinate expression is measured from the positive x-axis in the direction of rotation whereas the angle θ' in the rotating coordinate expression is measured from the line of centers in the direction of rotation. The assumptions used in the derivation of equations (1) and (2) include:

1. The fluid inertia terms in the Navier-Stokes equations have been neglected due to their small magnitude.
2. Body forces in the fluid film have been neglected.
3. The fluid viscosity is constant.
4. The flow in the radial direction has been neglected, that is, the short bearing approximation has been used.

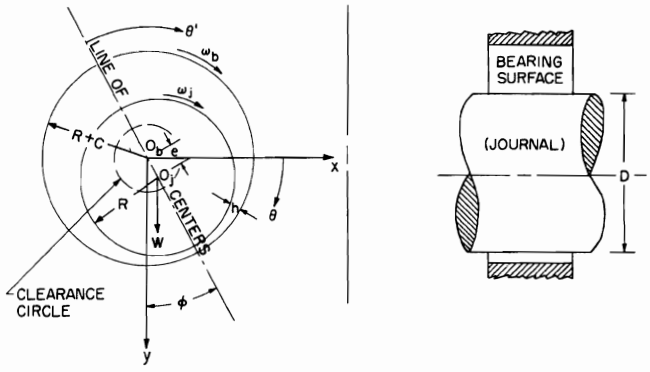

Figure 2-1. Squeeze Film Damper Bearing Configuration in Fixed and Rotating Coordinate Systems.

A comparison of the short bearing solution and the general solution of the Reynolds equation solved by a finite difference technique for the plain journal bearing under steady state conditions shows that the short bearing solution is highly accurate for a wide range of eccentricities for L/D < 1/4 and is acceptable for L/D values up to 1 if the eccentricity ratio is low. The normal design range of the squeeze film bearings will be L/D < 1/2 and eccentricity ratios < 0.4.

2.2 Bearing Forces in Fixed Coordinates

For the plain bearing with full end leakage the appropriate boundary conditions are:

$$P(\theta,0) = P(\theta,L) = 0 \qquad (2\text{-}3)$$

In the fixed coordinate system the film thickness, h, is given by:

$$h = c - x\cos\theta - y\sin\theta \qquad (2\text{-}4)$$

Substituting into equation (2-1) and integrating yields:

$$P(\theta,Z) = \frac{3\mu}{h^3}\left[Z^2 - LZ\right]\left[(\omega_b + \omega_j)\frac{\partial h}{\partial \theta} + 2\frac{\partial h}{\partial t}\right] \qquad (2\text{-}5)$$

The total force components in the x and y directions are found by integrating the pressure over the entire journal surface.

$$F_x = -\int_0^{2\pi}\int_0^{L} P(\theta,Z)\,R\cos\theta\,dZ\,d\theta \qquad (2\text{-}6)$$

$$F_y = -\int_0^{2\pi}\int_0^{L} P(\theta,Z)\,R\sin\theta\,dZ\,d\theta \qquad (2\text{-}7)$$

Substituting the expressions for $\partial h/\partial t$ and $\partial h/\partial\theta$ into the pressure equation and integrating around the bearing circumference gives:

$$\begin{Bmatrix} F_x \\ F_y \end{Bmatrix} = \frac{-\mu R L^3}{2}\int_0^{2\pi} \frac{(\omega_b + \omega_j)(x\sin\theta - y\cos\theta) - 2(\dot{x}\cos\theta + \dot{y}\sin\theta)}{(c - x\cos\theta - y\sin\theta)^3}\begin{Bmatrix}\cos\theta \\ \sin\theta\end{Bmatrix} d\theta \qquad (2\text{-}8)$$

The above equation is applicable to the evaluation of the forces developed in the plain journal bearing as well as the squeeze film damper bearing for arbitrary values of journal dispacement, velocity, and shaft and bearing housing angular velocities. Hence the analysis can also be used for the general floating bush bearing with rotation.

For the case of the squeeze film damper where the journal and housing are constrained from rotating, $(\omega_b = \omega_j = 0)$, expressions become

$$\begin{Bmatrix} F_x \\ F_y \end{Bmatrix} = \frac{-\mu R L^3}{2}\int_0^{2\pi} \frac{-2(\dot{x}\cos\theta + \dot{y}\sin\theta)}{(c - x\cos\theta - y\sin\theta)^3}\begin{Bmatrix}\cos\theta \\ \sin\theta\end{Bmatrix} d\theta \qquad (2\text{-}9)$$

These non-linear fluid film forces are easily combined with the rotor-bearing system dynamical equations providing a complete non-linear dynamical analysis of the system. Because

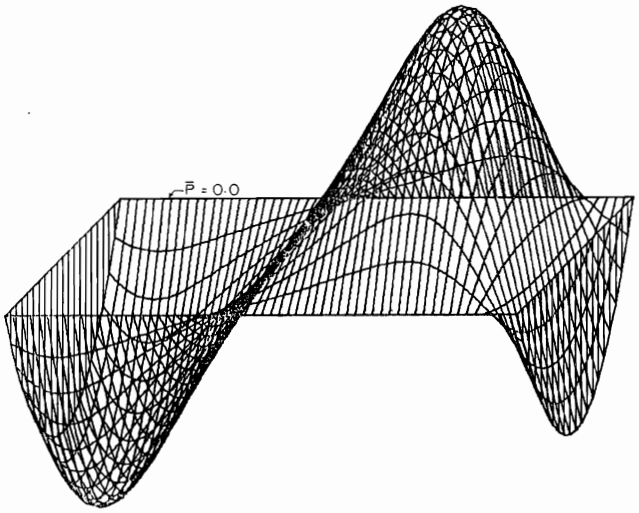

Figure 2-2. Uncavitated Pressure Profile Showing Region of Negative Hydrodynamic Pressure.

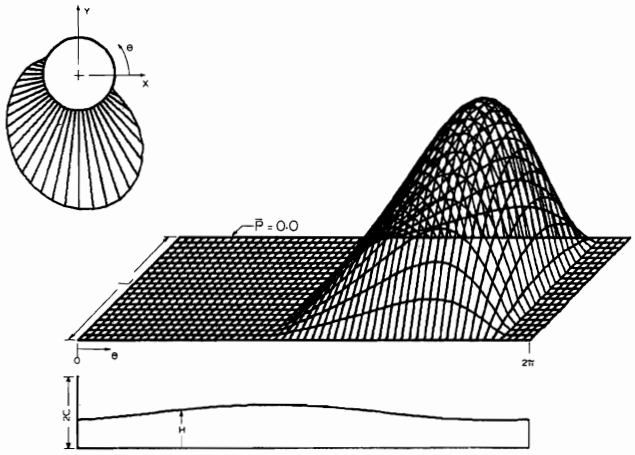

Figure 2-3. Cavitated Pressure Profile with Negative Hydrodynamic Pressure Equated to Zero.

the bearing force equations are written in fixed Cartesian coordinates a transformation from one coordinate system to another is not required. This is very important for conservation of computation time since the bearing pressure profile must be integrated at each time step of the system motion.

2.3 *Damper Cavitation*

If the complete pressure profile is calculated without regard to cavitation or rupture of the film, then the bearing pressure will be similar to Figure (2-2). This figure represents the three dimensional pressure generated in the bearing.

The exact mechanism causing cavitation in fluids is not fully known. It is known that film rupture is influenced by gas and solid content of the fluid. Recent investigations have shown that a fluid may stand large tensile stresses [2], and its ability to withstand rupture is dependent on its past history. In this investigation it is assumed that cavitation occurs when the pressure in the film drops below ambient pressure. The cavitated film then extends over only a section of the bearing circumference as shown in Figure (2-3). Recent experimental research has shown that cavitation in the squeeze bearing occurs in streamers of bubbles which extend around the entire bearing [3]. These streamers initially appear at the center of the bearing and extend outward as the rotor speed increases. It is beyond the scope of this present paper to analyze this type of cavitation effect. Therefore the conventional cavitated film is assumed to occur when $P<P_c$ where P_c is the assumed cavitation pressure.

When evaluating the integral of equation (2-9), negative pressures are equated to zero if the film is assumed to cavitate. If the oil supply pressure is sufficiently high and suitable operating conditions exist the film does not cavitate.

2.4 *Bearing Forces in Rotating Coordinates*

The Reynolds equation in rotating coordinates was given by equation (2-2). Assuming steady-state circular synchronous precession of the journal about the bearing center and no axial misalignment, equation (2-2) can be integrated in closed form. The resulting equations for the bearing forces give the equivalent stiffness and damping of the bearing.

The force components are:

$$\begin{Bmatrix} F_r \\ F_\theta \end{Bmatrix} = \frac{-\mu R L^3}{c^2} \int_{\theta_1'}^{\theta_2'} \frac{(\dot{\phi}\,\epsilon \sin\theta' + \dot{\epsilon}\cos\theta')}{(1+\epsilon\cos\theta')^3} \begin{Bmatrix} \cos\theta' \\ \sin\theta' \end{Bmatrix} d\theta' \tag{2-10}$$

The limits of integration, θ_1' and θ_2', define the area over which a positive pressure profile exists and are dependent on the type of journal motion and whether or not cavitation occurs.

It is assumed that the damper is precessing in steady-state circular motion about the origin and therefore $\dot{\epsilon} = 0$.

The resulting force components are:

$$F_r = \frac{-2\mu R L^3 \epsilon \omega e}{c^3 (1-\epsilon^2)^2} \tag{2-11}$$

and

$$F_\theta = \frac{-\mu R L^3 \pi e \omega}{2c^3 (1-\epsilon^2)^{3/2}} \tag{2-12}$$

The force in equation (2-11) appears as a stiffness coefficient times a displacement acting in line of the displacement towards the bearing center. The equivalent damper stiffness is:

$$K_0 = \frac{2\mu R L^3 \epsilon \omega}{c^3 (1-\epsilon^2)^2} \tag{2-13}$$

Since the journal is precessing and not rotating, every point in the journal has a velocity equal to $e\omega$. The force in equation (2-12) therefore appears as a damping coefficient times a velocity acting in the direction opposite the journal motion.

The equivalent damper damping is:

$$C_0 = \frac{\mu R L^3 \pi}{2c^3 (1-\epsilon^2)^{3/2}} \tag{2-14}$$

For the uncavitated film, the components are given by:

$$F_r = 0 \tag{2-15}$$

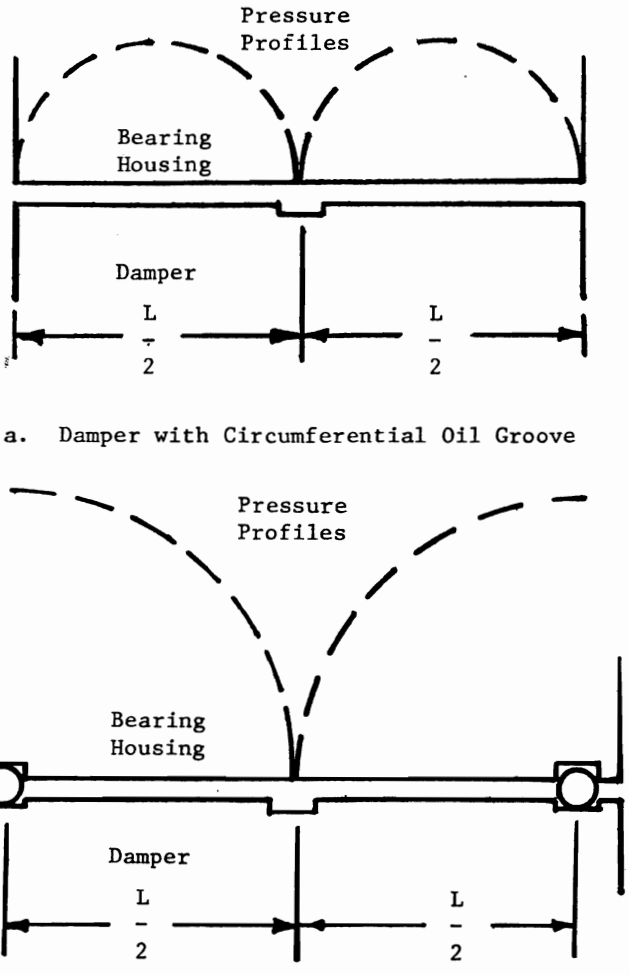

Figure 2-4. Dampers with Circumferential Oil Grooves and End Seals.

$$F_\theta = \frac{-\mu R L^3 \pi e \omega}{c^3 (1-\epsilon^2)^{3/2}} \qquad (2\text{-}16)$$

It is therefore evident that a complete fluid film does not produce an equivalent bearing stiffness but doubles the damping of the cavitated film.

Although the equations for the damper characteristics were derived for a plain damper, they are applicable to other damper configurations such as those shown in Figure 2.4. A damper with a circumferential oil groove and full end leakage, shown in Figure 2.4a, consists of two plain lands of length L/2. The pressure drops to atmospheric in the oil groove creating two parallel pressure profiles corresponding to two parallel dampers of length L/2. Thus the maximum pressure in each side of the damper is reduced a factor of four and the force on each side is reduced by a factor of eight. The net effect of cutting a circumferential oil groove in the damper is to decrease the hydrodynamic force and both bearing coefficients by a factor of four.

The damper represented in Figure 2.4b has a circumferential oil groove and end seals to prevent end leakage. Since the pressure vanishes at the center, the pressure profile is equivalent to that for a plain land without an oil groove and without end seals. The values for total force, stiffness, and damping are also the same.

As will be shown in later sections, it is often desired to design a damper to have stiffness and damping values within a certain range. The amount that the clearance can be increased may be limited by sealing or other conditions which necessitates lowering the damper characteristics by other means. Circumferential grooves serve to lower both stiffness and damping of the damper without changing the distance between the end seals. The characteristics can be easily calculated by summing the effects of the lands between the oil grooves.

The damper equations derived in this section are summarized in Table (2-1). Also included in the table are the equations for pure radial squeeze motion. For this type of operation $\phi \cdot = o$ and results from a purely unidirectional load on the journal. The radial and tangential force components are derived from equation (2-10) where only the term containing ϵ° in the integral is retained. The pressure equation is also modified to include only the ϵ° term. The maximum pressure occurs at $\theta' = \pi$ for all values of journal eccentricity. Examination of the pressure equation reveals that the hydrodynamic pressure is positive only in the region $\theta' = \pi/2$ to $3/2\pi$. These values of θ' are the limits of integration in equation (2-10) for the cavitated film.

TYPE OF MOTION	MAXIMUM PRESSURE	EQUIVALENT DAMPING Ko (lb/in)	EQUIVALENT DAMPING Co (lb-sec/in)
CIRCULAR SYNCHRONOUS PRECESSION $\dot{\phi} = \omega,\ \dot{\epsilon} = 0$ CAVITATED FILM	$\frac{-3\mu L^2 \omega \epsilon \sin\theta_m}{2c^2(1+\epsilon\cos\theta_m)^3}$ where θ_m is given by:	$\frac{2\mu R L^3 \epsilon \omega}{c^3(1-\epsilon^2)^2}$	$\frac{\mu R L^3}{2c^3(1-\epsilon^2)^{3/2}}\pi$
UNCAVITATED FILM	$(1+\epsilon\cos\theta_m)\cos\theta_m + 3\epsilon\sin^2\theta_m = 0$	0	$\frac{\mu R L^3}{c^3(1-\epsilon^2)^{3/2}}\pi$
PURE RADIAL SQUEEZE MOTION $\dot{\phi} = 0,\ \dot{\epsilon} \neq 0$ CAVITATED FILM	$\frac{-3\mu L^2 \dot{\epsilon} \cos\theta_m}{2c^2(1+\epsilon\cos\theta_m)^3}$ $\theta_m = \pi$	0	$\frac{\mu R L^3 [\pi - \cos^{-1}(\epsilon)](2\epsilon^2+1)}{c^3(1-\epsilon^2)^{5/2}}$
UNCAVITATED FILM		0	$\frac{\mu R L^3 \pi (2\epsilon^2+1)}{c^3(1-\epsilon^2)^{5/2}}$

Table 2-1. Summary of Equivalent Stiffness and Damping Coefficients for Squeeze Film Damper Bearings.

The table also shows that for purely radial motion no damper stiffness is obtained in either the cavitated or uncavitated damper. Thus if this type of motion exists retainer springs must be included to provide support flexibility.

For the case of circular damper precession, the table shows the stiffness and damping of the cavitated film and damping of the uncavitated film remain essentially constant for low eccentricity ratios. As the eccentricity ratio increases above 0.4 there is a rapid increase in these properties and they approach infinity as ϵ approaches 1. This variation of stiffness in the cavitated film is very important. As the eccentricity becomes large the support becomes more rigid with a corresponding increase in the rotor critical speed. If the rotor critical speed is increased above the operating speed, the phase angle between the rotor unbalance vector and amplitude vector becomes less than 90°. When this condition occurs the force transmitted through the support structure will always be greater than the unbalance load. With an uncavitated film this problem does not occur because no damper stiffness is generated. To obtain the stiffness required to stabilize a rotor (see Section 3) it is necessary to use retainer springs in the support bearings.

One of the most significant parameters affecting damper performance is the length to clearance ratio. The stiffness and damping coefficients vary as $(L/C)^3$ and therefore either doubling the bearing length or decreasing the clearance by 1/2 will increase the coefficients by a factor of 8.

3. ROTOR-BEARING STABILITY AND DAMPER ANALYSIS

3.1 Rotor-Bearing Stability

After Jeffcott's [5] analysis in 1919 of the single mass flexible rotor on rigid bearings, manufacturers began producing light, flexible rotors operating above the first critical speed. However some manufacturers encountered severe operating difficulties with some of their designs. These machines underwent violent whirling while running above the critical speed and often failed.

Experimental and analytical investigations by Newkirk and Kimball [6] [7] revealed that the whirl instability was not caused by unbalance in the rotor, but by internal shaft effects such as internal friction. Kimball theorized that forces normal to the plane of the deflected rotor could be produced by alternating stresses in the metal fibers of the shaft. In light of this theory, Newkirk concluded also that the same normal forces could be produced by shrink fits on the rotor shaft. By incorporating these forces in Jeffcott's model Newkirk showed that the rotor could be unstable above the rotor critical speed.

Further investigation by Newkirk showed cases of rotor instability which were not produced by shaft effects but by effects in the journal bearings [8]. One cause of journal bearing instability was later shown to be due to lack of radial stiffness in the bearing and the instability occurred at twice the rotor critical speed. These instabilities were especially common in lightly loaded rotors and larger bearing loads tended to promote stability. The effect of the larger loads is to cause cavitation of the fluid film which results in a radial stiffness component of the bearing forces being produced [9], [10], [11].

In 1965 Alford reported on the effects of aerodynamic forces on rotors [12]. He showed that these forces couple the rotor equations of motion and can produce instability. He also noted that labyrinth seals and balance pistons also produce forces that can promote instability.

Recent investigators including Gunter, Kirk and Choudhury [13], [14], [15] have analyzed the effects of support flexibility and damping on reducing rotor instability produced by the forces just described. As a result they have derived stability criteria for determining the necessary support characteristics.

One of the most general methods for determining rotor stability is to derive the characteristic frequency equation of the system. The stability is given by the roots of this equation. The real part of the root corresponds to an exponentially increasing or decreasing function of time. Thus a positive real part indicates instability whereas a negative real part indicates a stable system. This type of stability analysis of a rotor-bearing system therefore requires that the characteristic equation be known. This equation is not always easy to obtain.

The characteristic equation is derived from the homogeneous second order differential equations of motion of the system [15]. By assuming solutions of the form

$$x_i = A_i e^{\lambda t} \qquad i = 1, 2, \ldots, n$$

and differentiating, the equations are substituted back into the equations of motion. This produces a matrix known as the characteristic matrix. The determinant of this matrix gives the characteristic equation, a polynomial of degree 2n in λ, where n is the number of degrees of freedom of the system.

The computer program SDSTB [16] was used to produce the stability maps shown in this section. The program calculates the characteristic equation for a three-mass symmetric flexible rotor mounted in journal bearings and supported in squeeze film damper bearings. The rotor-bearing model is shown in Figure (3-1). The rotor is assumed to remain stationary in the axial direction so the rotor has six degrees of freedom and the characteristic equation is therefore of degree twelve. The characteristic matrix is shown in Figure (3-2). The determinant of this matrix gives the characteristic equation. The unknown variable in this equation is λ, the natural frequency of the system. An examination of the characteristic matrix shows that the coefficients of λ are functions of the rotor and bearing properties as well as internal shaft friction, absolute rotor damping and aerodynamic cross coupling. The natural frequencies and stability of the system are found by finding the roots of this equation.

The journal and support bearing characteristics can either be inserted directly as linear coefficients or they may be calculated in the program from the bearing parameters by solving for the equilibrium positions of the journal and support. These characteristics are non-linear functions of the journal eccentricity. The stability maps in this chapter were produced with the linearized journal and support bearing characteristics given as input data to the program. The assumption of linear bearing characteristics is useful because for low eccentricity the characteristics do not vary greatly with changes in eccentricity. This assumption allows a large savings in computer time. If the non-linear characteristics are calculated, the amount of computer time increases because an iterative procedure is used to find the equilibrium position.

As an example of how a stability map is produced, consider the following system:

ROTOR CHARACTERISTICS

ROTOR WEIGHT	W2	=	675 lbs
JOURNAL WEIGHT	WJ	=	312 lbs (each)
SUPPORT WEIGHT	W1	=	15 lbs (each)
SHAFT STIFFNESS	KS	=	280,000 lb/in
SHAFT DAMPING	CS	=	.10 lb-sec/in
INTERNAL DAMPING	CI	=	0.0 lb-sec/in
ROTOR SPEED	N	=	10,000 RPM

BEARING CHARACTERISTICS

K_{xx}	=	1.287×10^6 lb/in
K_{yy}	=	1.428×10^6 lb/in
C_{xx}	=	1200 lb-sec/in
C_{yy}	=	1290 lb-sec/in
$K_{xy} = K_{yx}$	=	0.0 lb/in
$C_{xy} = C_{yx}$	=	0.0 lb-sec/in

Two values of aerodynamic cross coupling were selected, Q=20,000 lb/in and Q=100,000 lb/in. For each value of Q,

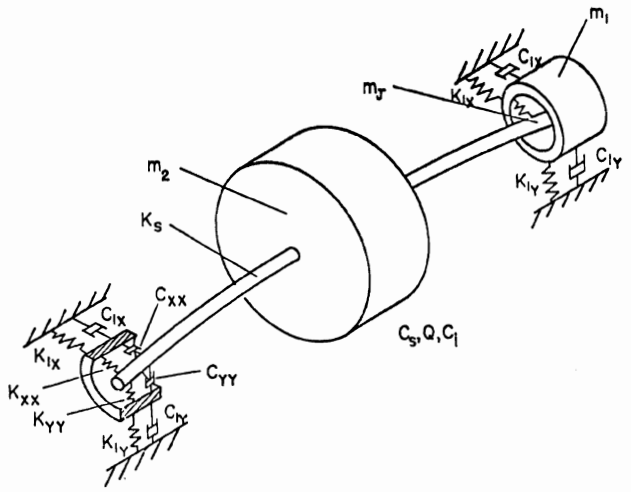

Figure 3-1. Three-Mass Flexible Rotor Mounted in Flexible, Damped Supports

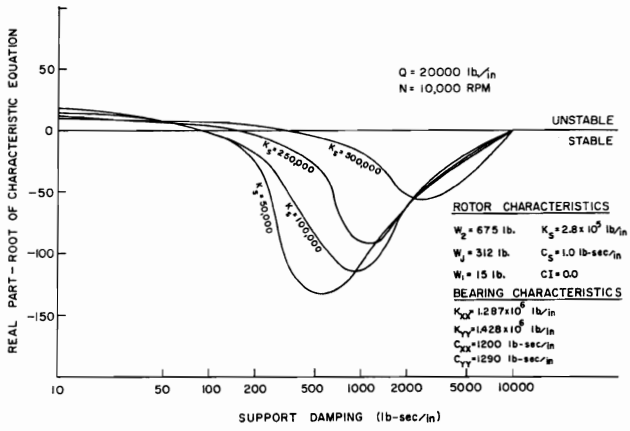

Figure 3-3. Stability of a Flexible Rotor with Aerodynamic Cross-Coupling (Q=20,000 lb/in, N=10,000 RPM).

several values of support stiffness were selected ranging from 50,000 lb/in to 500,000 lb/in. For each value of support stiffness a range of support damping values from 0 to 10,000 lb-sec/in was used. Using this method a stability contour was found for a given value of aerodynamic cross coupling and support stiffness. The rotor and bearing characteristics remained unchanged.

Figures (3-3) and (3-4) show the stability maps for the above system for the two values of aerodynamic cross coupling.

There is an intermediate range of support damping values for which the system is stable for a given value of the support stiffness. As the stiffness is increased the system becomes less stable. With Q=20,000 lb/in the optimum amount of damping ranges from 500 to 2,500 lb-sec/in as the stiffness increases from 50,000 to 500,000 lb/in. For damping less than 100 lb-sec/in the system is unstable for all values of stiffness. The same is true if the damping exceeds 10,000 lb-sec/in.

For Q=100,000 lb/in the optimum damping is 1,000 lb-sec/in and does not shift over the stiffness range selected. When the support stiffness reaches 250,000 lb/in the system is unstable for all values of damping.

$$
\begin{array}{l}
x_2: \\
y_2: \\
x_J: \\
y_J: \\
x_b: \\
y_b:
\end{array}
\begin{bmatrix}
m_2\lambda^2 + (IC+cs)\lambda + k_s & Q+\omega IC & -\lambda IC - k_s & -\omega IC & 0 & 0 \\
-Q-\omega IC & m_2\lambda^2 + (IC+cs)\lambda + k_s & \omega IC & -\lambda IC - k_s & 0 & 0 \\
-\lambda IC/2 - (k_s+\omega IC)/2 & 0 & m_J\lambda^2 + (c_{xx}+IC/2)\lambda + (k_s+\omega IC)/2 + k_{xx} & c_{xy}\lambda + k_{xy} & -c_{xx}\lambda - k_{xx} & -c_{xy}\lambda - k_{xy} \\
0 & -\lambda IC/2 - (k_s-\omega IC)/2 & c_{yx}\lambda + k_{yx} & m_J\lambda^2 + (c_{yy}+IC/2)\lambda + (k_s-\omega IC)/2 + k_{yy} & -c_{yx}\lambda - k_{yx} & -c_{yy}\lambda - k_{yy} \\
0 & 0 & -c_{xx}\lambda - k_{xx} & -c_{xy}\lambda - k_{xy} & m_b\lambda^2 + (c_{xx}+c_{1xx})\lambda + (k_{xx}+k_{1xx}) & (c_{xy}+c_{1xy})\lambda + (k_{xy}+k_{1xy}) \\
0 & 0 & -c_{yx}\lambda - k_{yx} & -c_{yy}\lambda - k_{yy} & (c_{yx}+c_{1yx})\lambda + (k_{yx}+k_{1yx}) & m_b\lambda^2 + (c_{yy}+c_{1yy})\lambda + (k_{yy}+k_{1yy})
\end{bmatrix}
\begin{bmatrix} A_1 \\ A_2 \\ A_3 \\ A_4 \\ A_5 \\ A_6 \end{bmatrix}
=
\begin{bmatrix} 0 \\ 0 \\ 0 \\ 0 \\ 0 \\ 0 \end{bmatrix}
$$

Figure 3-2. Characteristic Matrix for Three-Mass Model Including Aerodynamic Cross-Coupling Internal Shaft Friction and Absolute Shaft Damping.

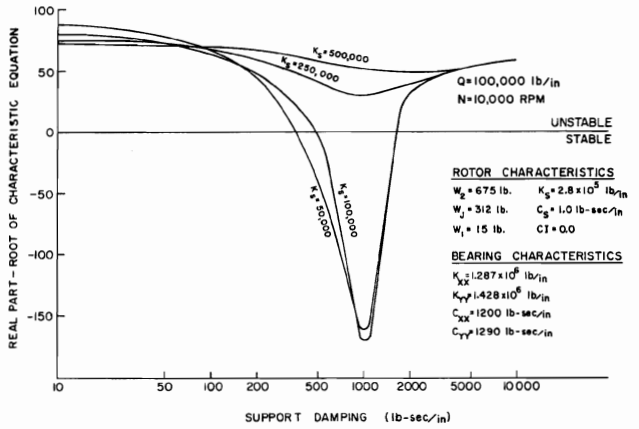

Figure 3-4. Stability of a Flexible Rotor with Aerodynamic Cross-Coupling (Q=100,000 lb/in, N=10,000 RPM).

3.2 Steady-State Analysis

The linearized stability maps just discussed provide information on the support characteristics needed to promote stability in a given rotor-bearing system. There remains the problem of relating these characteristics to the actual damper system. The squeeze bearing equations derived in section 2 in

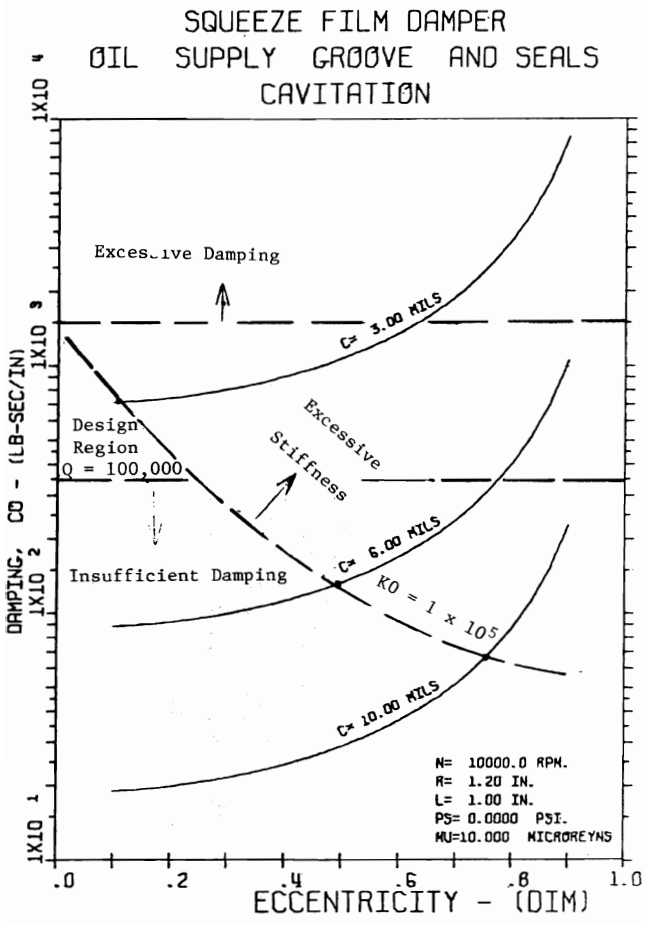

Figure 3-5. Damping Coefficient for Squeeze Film Bearing with Cavitated Film — End Seals and Oil Supply Groove Included.

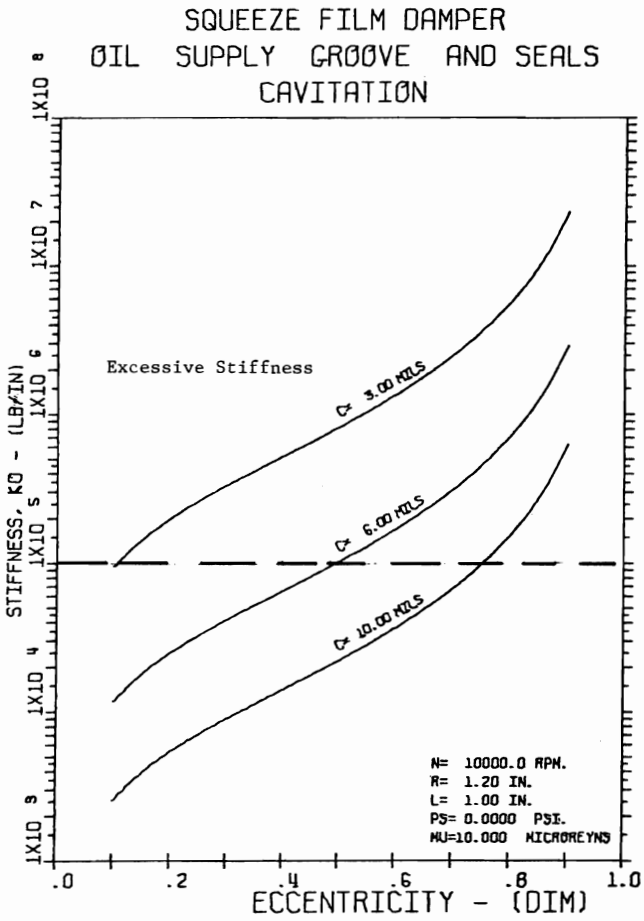

Figure 3-6. Stiffness Coefficient for Squeeze Film Bearing with Cavitated Film — End Seals and Oil Supply Groove Included.

rotating coordinates are used to determine the preliminary bearing design. As noted in section 2, these equations were derived assuming steady-state circular, synchronous precession of the journal.

The damper characteristics, stiffness, damping and pressure are functions of the amplitude of the journal orbit, fluid viscosity and damper geometry. The addition of oil supply grooves, end seals and cavitation affect the damper characteristics.

The steady-state equations have been programmed on a digital computer. This program, SQFDAMP, analyzes three basic bearing configurations:

1. Plain damper no oil supply groove or end seals.
2. Damper with oil supply groove but without end seals.
3. Damper with both oil supply groove and end seals.

Both cavitated and uncavitated fluid films can be analyzed.

Figures (3-5) — (3-7) show the characteristics for a damper being considered for the 675 lb. rotor system described earlier. The damper has an oil supply groove and end seals, and the fluid film is assumed to be cavitated. The damper parameters are, length 1.0 inches, radius 1.2 inches and fluid viscosity 10 microreyns.

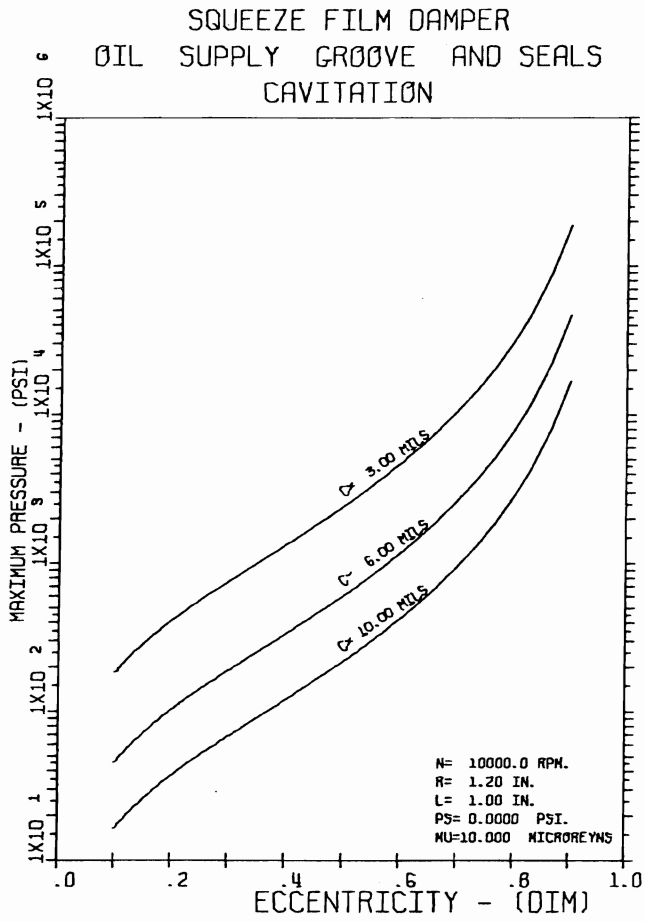

Figure 3-7. Maximum Pressure for Squeeze Film Bearing with Cavitated Film — End Seals and Oil Supply Groove Included.

For the case where Q=20,000 lb/in it was determined that the optimum support damping is about 500 lb-sec/in, and the support stiffness should be less than 100,000 lb/in. Because it is desirable to keep the eccentricity ratio of the damper low, Figures (3-5) and (3-6) reveal that this damper will provide the necessary stiffness and damping characteristics with a clearance of about 4 mils at an eccentricity ratio of ϵ=.10 to .20. This corresponds to a damper orbit of 0.4 to 0.8 mils amplitude. The maximum hydrodynamic pressure in the damper is about 100 psi for this clearance. If the fluid film does not cavitate, the resulting damping characteristics are doubled. A slightly larger clearance, 5.0 mils, will produce the optimum damping. However, because the uncavitated film does not produce an equivalent stiffness, retainer springs must be incorporated in the damper. If the end seals are flexible, the required spring rate may be obtained from them.

One advantage of the uncavitated film is that if the journal eccentricity ratio should become very large, there is no rise in stiffness that could cause the system to become unstable or raise the critical speed above the operating speed.

If Q=100,000 lb/in, the optimum damping is 1,000 lb-sec/in, and the effective damper stiffness developed by the combined acting of the retainer spring support and the damper hydrodynamic action cannot exceed 100,000 lb/in. In order to achieve the necessary damping required, a low clearance damper of the order of 3 to 4 mils is needed. However, since the total support stiffness cannot exceed 100,000 lb/in, then with a 3 mil clearance, the eccentricity of the damper cannot exceed 0.15 mil. With a 3 mil clearance and the damper operating with a synchronous orbit of ϵ=0.23 about the damper origin, a stiffness of 250,000 lb/in will be generated. This high value of stiffness therefore will prevent the rotor system from achieving stabilization.

If the aerodynamic cross-coupling on the machine is 100,000 lb/in, then the squeeze film damper must be sized very carefully for the application because of the large aerodynamic loading on the machine. For example, on Figure 3.6 a line is drawn at the stiffness value of 100,000 lbs/in. The damper cannot be operating above this level because of the excessive stiffness that would be generated by the damper. The intersection of the stiffness value of 100,000 with the clearance curves of 3, 6, and 10 mils produces the maximum allowable operating eccentricity for this design of damper. On Figure (3-5), the line of 1,500 is drawn on the figure. The operation of the damper cannot be above this level as this would produce excessive damping in the system. Likewise the line at 350 is drawn on the figure, and the damper cannot operate below this limit as there would be insufficient damping produced in order to stabilize the rotor. Thus the damper must operate so as to produce a range of damping coefficients between 350 and 1,500 lb-sec/in if the rotor is to be stabilized with this high value of aerodynamic cross-coupling. Next the points of intersection from Figure 3.6 where the stiffness line of 100,000 lb/in intersects the clearance curve is superimposed on Figure 3.5, and this line is drawn. The operation above this line will produce excessive stiffness in the damper. The region bounded by the excessive stiffness line and the damping lines produces the allowable design region. For this case of damper under consideration, it can be seen that there is only a small allowable design region between 2½ to 4 mils bearing clearance with a maximum eccentricity of .2. If the damper does not operate in this region, then proper stabilization of the rotor configuration will not be achieved. If the damper system is to be designed to stabilize a Q value of 100,000 lbs/in, it is therefore desirable to study other damper lengths and clearance values in order to obtain a damper configuration which has a larger design region. If the Q value for design is only required to be 20,000 lbs/in, then the design region is greatly extended, and the permissible damper clearance can vary from 3 to 6 mils with a maximum eccentricity of 2.6.

4. ROTOR TRANSIENT ANALYSIS

In the previous section, the design characteristics of the damper were presented based upon linearized rotor bearing theory. It is often important to evaluate the rotor dynamical behavior with and without a squeeze film damper under operating conditions. In order to gain an understanding of the type of rotor motion generated in the system under the action of aerodynamic cross-coupling or internal rotor friction, the rotor, as illustrated in the sample problem, was run with a transient program to simulate the motion at the rotor center and the bearing locations.

Figure 4.1 represents the journal motion of a turborotor mounted in tilting pad bearings operating at 10,000 RPM. The rotor mass center has a small unbalance of .5 mils eccentricity. The rotor is operating with an internal friction factor of 20 lb-sec/in. The behavior of the rotor is similar to the case when Q equals 20,000 lb/in. If noncontacting probes were placed at the bearing locations to monitor the rotor motion, there would

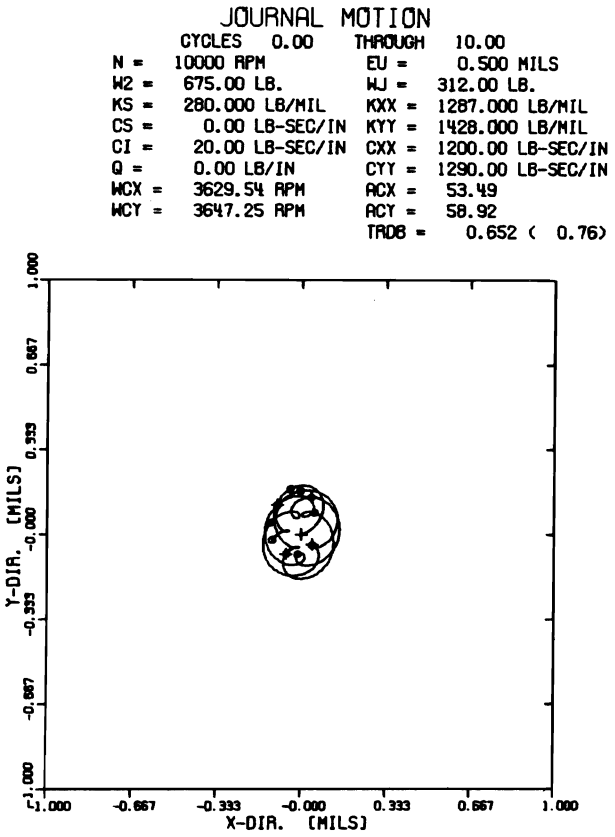

Figure 4-1. Tilting Pad Journal Motion at 10,000 RPM with Self-Excited Orbit due to Internal Friction (C_i=20).

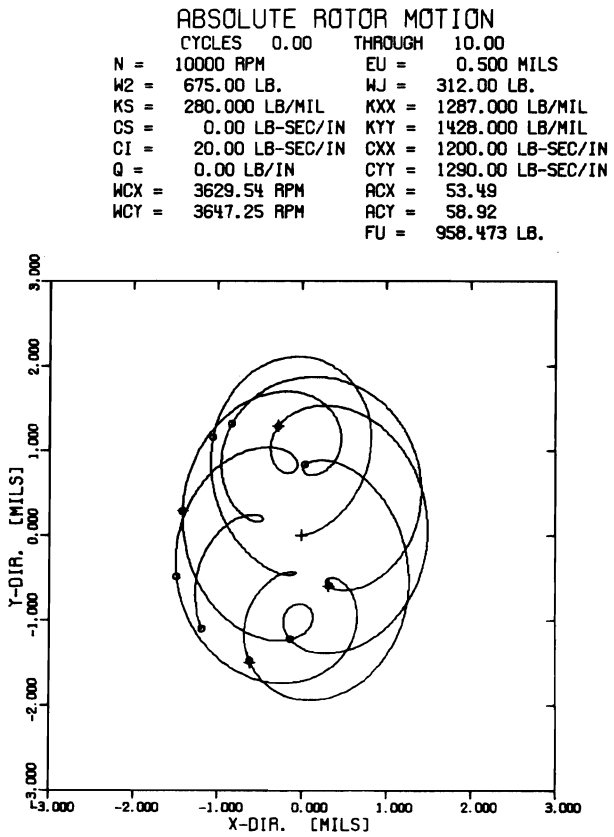

Figure 4-2. Rotor Center Motion at 10,000 RPM with Large Self-Excited Whirl Orbit (C_i=20).

probably be little reason for concern as the total rotor amplitude is approximately 1/2 of a mil. A frequency analyzer, however, would indicate that there is a fractional frequency whirl motion present in the journal orbit.

However, if noncontacting probes were placed at the rotor center, then a large whirl orbit of over 4 mils would be detected as shown in Fig. 4.2. Therefore, it is seen that the rotor motion is 8 times the magnitude of the bearing motion for this particular configuration. Even if the rotor speed increases while the aerodynamic cross-coupling or internal friction remains constant, then the whirl amplitude will greatly increase. Sustained rotor operations under these conditions could result in the contacting of the rotating element with the casing with possible dire consequences.

Figure 4.3 represents the rotor system with a squeeze damper support system added to it with a design support stiffness of 130,000 lb/in and a support damping of 150 lb-sec/in. The rotor speed is also taken as 10,000 RPM. The rotor system is released, and the centerline rapidly spirals out from the origin due to the application of the rotor unbalance. After approximately 10 cycles of shaft motion, the initial transient motion dies out, and the rotor assumes a stable synchronous whirl orbit with a maximum amplitude of 1 mil. Figure 4.4 represents the rotor motion with the speed increased to 16,000 RPM. The absolute rotor orbit shown in the figure represents the trajectory from 10 to 18 cycles of shaft motion. Here again it can be seen that the rotor is approaching a highly stable synchronous whirl orbit. In Figures 4.3 and 4.4 it is seen that the rotor under the action of low internal friction or aerodynamic cross-coupling can be stabilized with a damping value as low as 150 lb-sec/in. However, if the damping vale chosen for the

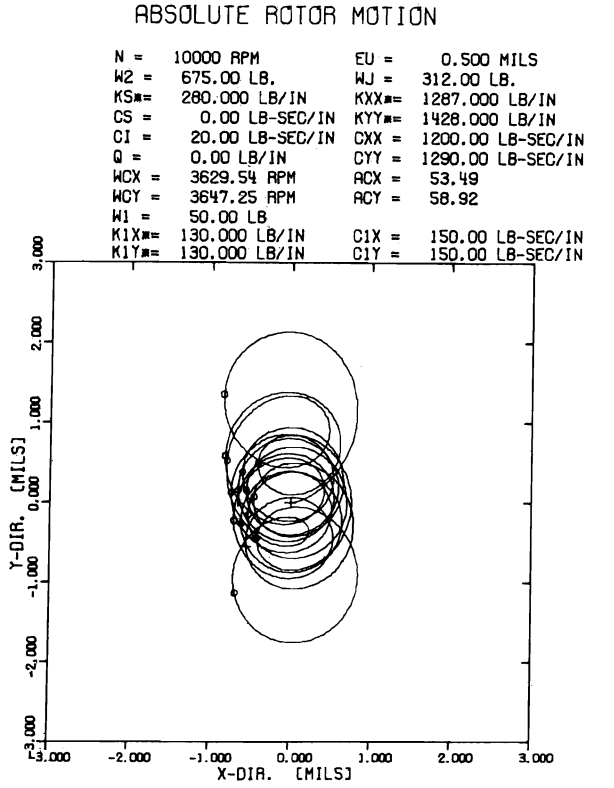

Figure 4-3. Stabilized Motion with Damper Support at 10,000 RPM (C_i=20, K_1=130,000 lb/in, C_1=150 lb-sec/in).

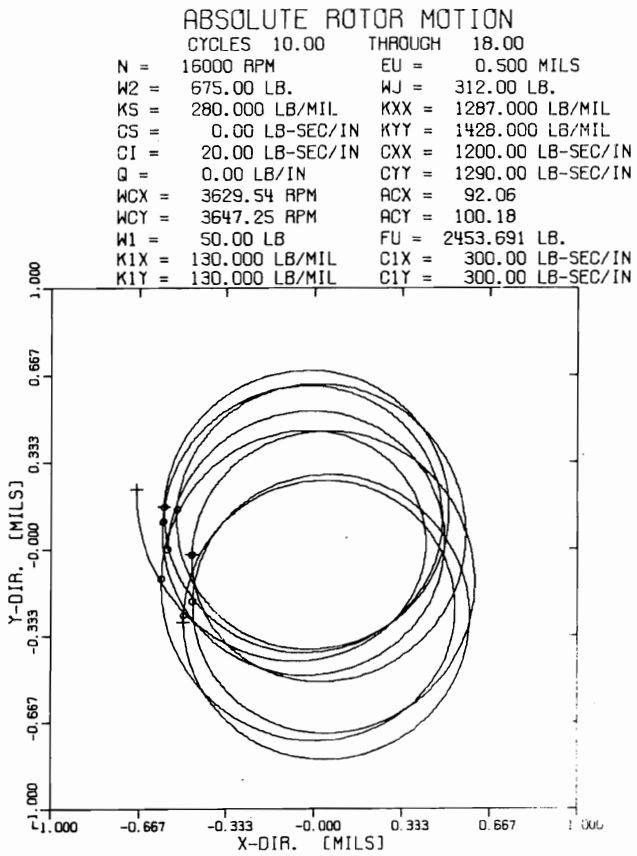

Figure 4-4. Stabilized Compressor Motion at 16,000 RPM with Damper Support (C_I=20, K_I=130,000 lb/in, C_I=300 lb-sec/in).

damper is too low, the rotor is unstable. Figure 4.5 shows several orbits of the rotor with 50,000 lb/in stiffness, but only 10 lb-sec/in damping. This underdamped system goes unstable rapidly.

Figure 3.4 on the stability of the flexible rotor with the large aerodynamic cross-coupling of Q=100,000 lb/in shows that in order to stabilize the rotor, the support system must be carefully tuned with a support damping of 1,000 lb-sec/in and a support stiffness of the range of 50,000 to 100,000 lb/in. Figure 4.6 represents the rotor motion with an aerodynamic cross-coupling of Q=100,000 lb/in and the optimum support characteristics of K=50,000 lb/in and a support damping of 1,000 lb-sec/in. It can be seen that after the initial transient motion has died out the rotor orbit is a highly stable synchronous motion with an amplitude of approximately 1.2 mils. If the damper should be overloaded in the vertical direction due to external loads and improper centering, then it is possible for the damper stiffness to increase greatly in excess of the 50,000 lb/in optimum value. Figure 4.7 represents the situation similar to Figure 4.6 except that the vertical support stiffness has been increased from 50,000 to 500,000 lb/in. In this case it can be seen that the rotor motion is highly unstable, and the rotor continues to orbit outward with a large self-excited whirl motion. After five cycles of shaft motion, the orbit has grown to over 7 mils amplitude in the vertical direction.

The transient rotor and damper motion presented in the previous figures was based upon linearized bearing and damper coefficients. In the actual damper, the forces generated are

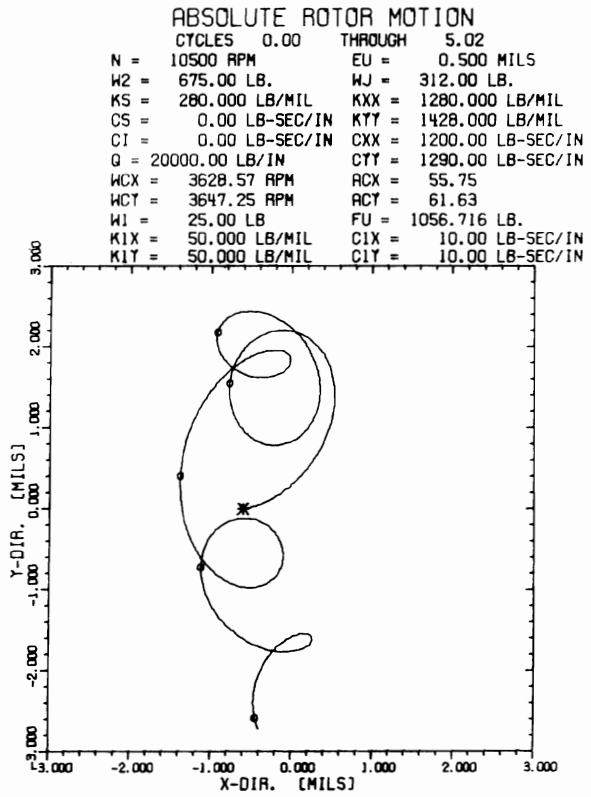

Figure 4-5. Unstable Compressor Motion with Low Aerodynamic Cross-Coupling — Underdamped Support.

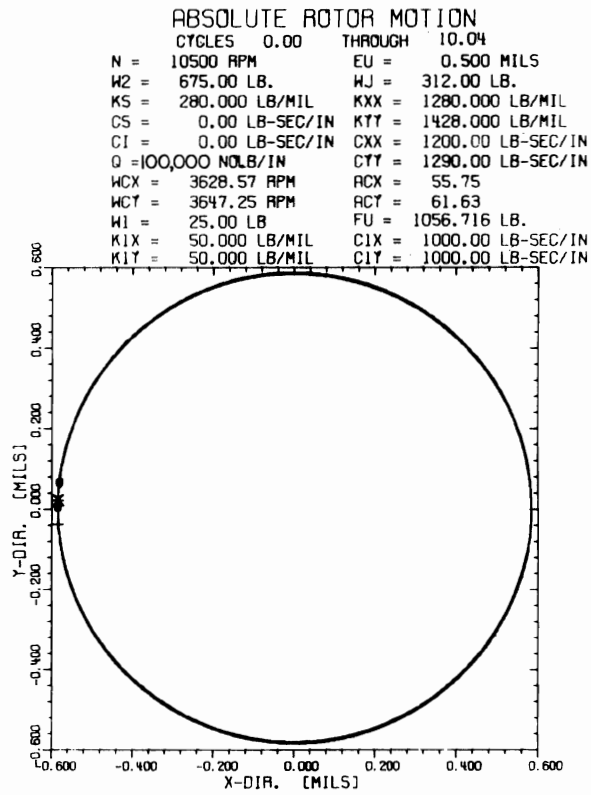

Figure 4-6. Stabilized Compressor Motion at 10,500 RPM with High Aerodynamic Cross-Coupling with Optimum Support Damping.

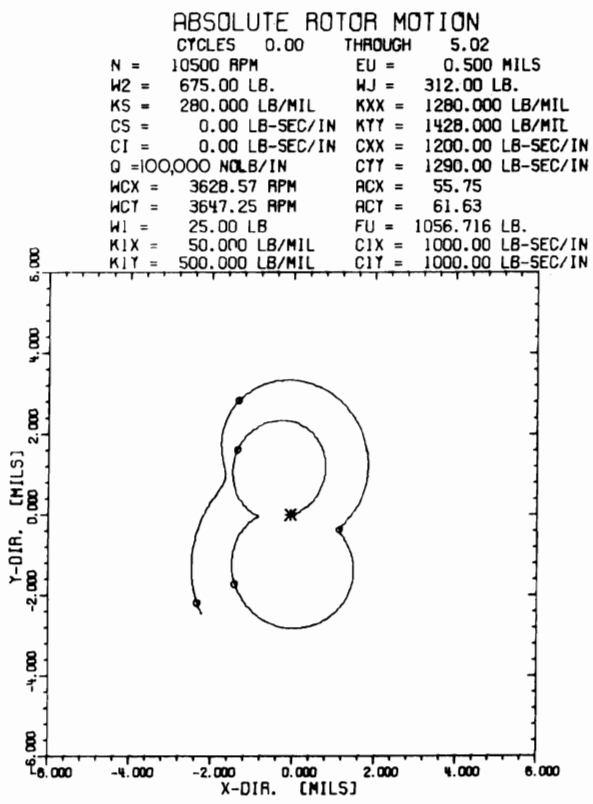

Figure 4-7. Unstable Compressor Motion at 10,500 RPM with High Aerodynamic Cross-Coupling — Excessive Support Stiffness.

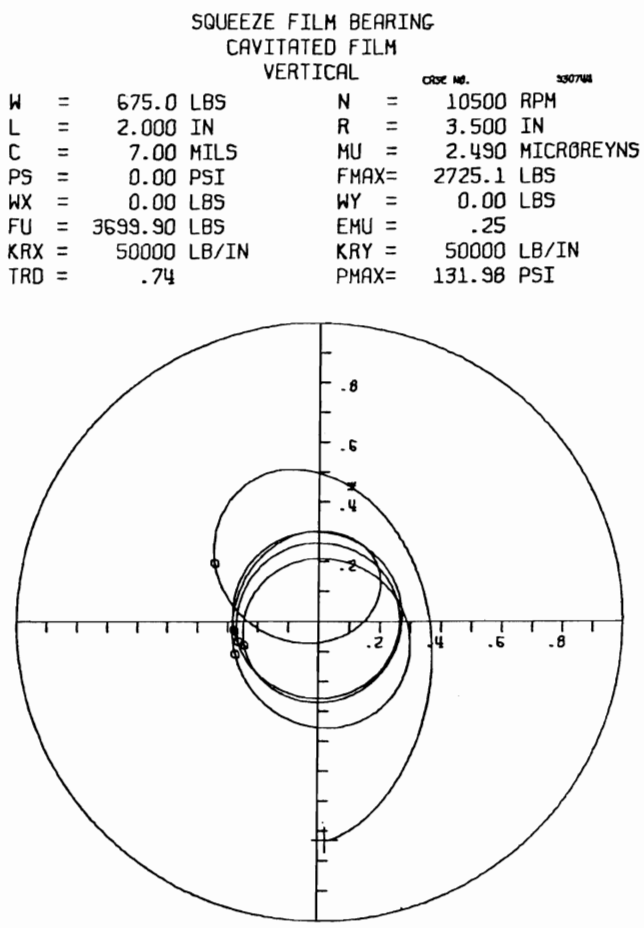

Figure 4-8. Vertical Unbalanced Rotor in Squeeze Film Bearing — Effect of Unbalance Magnitude — Unbalance Eccentricity — 1.75 Mils.

highly nonlinear functions of the journal displacement and velocity components. In order to take this into consideration, transient orbits of the rotor bearing system were run using the complete nonlinear damper forces in the program. It has been found that the unbalance level, centering and the magnitude of the retainer spring rate have a significant effect on the ability of the damper to perform properly. For example, Figure 4.8 represents the motion of the squeeze film damper with a retainer spring of 50,000 lb/in and a clearance of 7 mils. The rotor has an unbalance eccentricity of 25% of the bearing clearance of 1.75 mils, which creates a rotating load of 3,700 lbs. Although the initial starting position assumed was considerably removed from the final steady-state orbit, it can be seen that the initial transient quickly dies out and the damper assumes a synchronous circular orbit with an eccentricity of radius of .25. The maximum dynamic transmissibility encountered was .74 which occurred during the first cycle of shaft motion. After the steady-state motion is achieved, the final dynamic transmissibility is greatly reduced and is of the order of .37. Therefore it can be seen that the squeeze film damper, in addition to stabilizing the rotor motion also greatly assists in the attenuation of the forces generated by rotor unbalance.

If the squeeze damper were perfectly linear, a doubling of the unbalance force would cause twice the force transmitted to the support system. However, the dynamic transmissibility of .37 would remain the same. In Figure 4.9, the unbalance eccentricity is increased from .25 to .5. Here it is seen that the dynamic transmissibility has increased dramatically from .74 to 2.15. This implies that more force is transmitted through the damper support system than there would be if the damper were perfectly rigid. This represents a situation where putting in a damper is worse than putting in no damper at all. Therefore it is seen that if the rotor is operating with high unbalance as well as aerodynamic cross-coupling, the nonlinear forces generated in the squeeze film damper would be such that the high equivalent damper stiffness generated would not permit the damper support system to stabilize the rotor.

5. *EXPERIMENTAL ROTOR MOTION*

The squeeze film damper bearing has been applied successfully to several centrifugal compressors in order to stabilize them from self-excited whirl motion. However in each case, the squeeze film damper bearing had to be carefully sized for the particular machine in consideration. The design of the squeeze film damper for one machine may not necessarily produce satisfactory results in another. Figure 5.1 represents a centrifugal compressor before and after stabilization with a squeeze film damper. The trace at the left represents the original orbit of the rotor operating at a compressor discharge pressure of 175 psi. The rotor became highly unstable above this discharge of pressure. After the squeeze film damper was employed, the full compressor discharge pressure could be achieved. The resulting whirl orbit as shown in the right hand upper figure shows that the rotor system is highly stable with only a small component of self-excited whirl motion existing in the rotor.

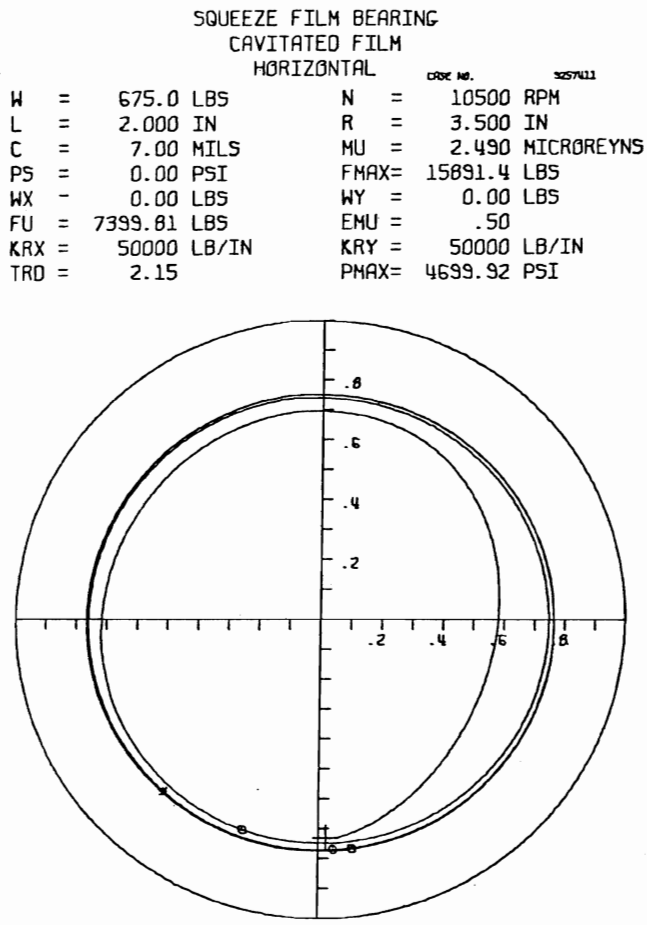

Figure 4-9. Vertical Unbalanced Rotor in Squeeze Film Bearing — Effect of Unbalance Magnitude — Unbalance Eccentricity=3.50 Mils.

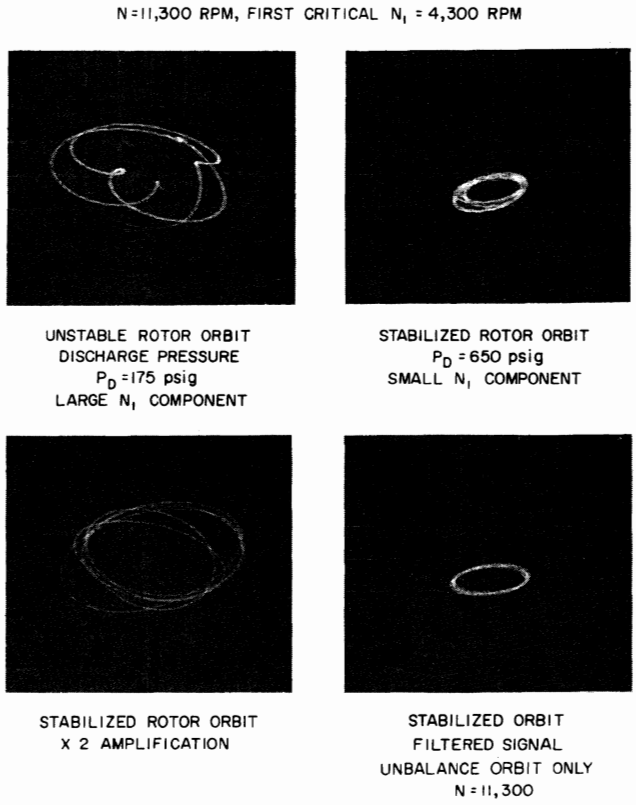

Figure 5-1. Rotor Orbits of a Turbo Compressor Before and After Stabilization by Damper Supports.

Figure 5.2 represents the frequency spectrum for various operating speeds of a centrifugal compressor in tilting pad bearings which exhibited whirl instability at the design operating speed. The rotor was run from 0 to 14,000 RPM, and the motion was recorded on tape and analyzed through a real time analyzer. At the various speeds, an analysis was made of the frequency components of the rotor motion. For example, the 45° line drawn on the plot represents the synchronous rotor motion. There is also a small component of twice the operating speed as seen on the chart. At a speed of 10,500 RPM a small component of self-excited whirl instability was detected. The frequency of this component corresponds approximately to the first critical speed at 4,200 RPM. As the speed of the rotor is increased, the subsynchronous whirl motion grows. Operation under these conditions caused a considerable wearing of the seals and bearings which required periodic replacement of the components.

Squeeze film dampers were designed for this compressor using the methods developed in the previous sections. Figure 5.3 represents the frequency spectrum of the compressor with the squeeze film dampers installed. Note that the rotor system is now highly stable and that there is no indication of self-excited whirl instability. The synchronous motion at design speed was also reduced considerably by means of trim balancing a coupling. It should be noted that

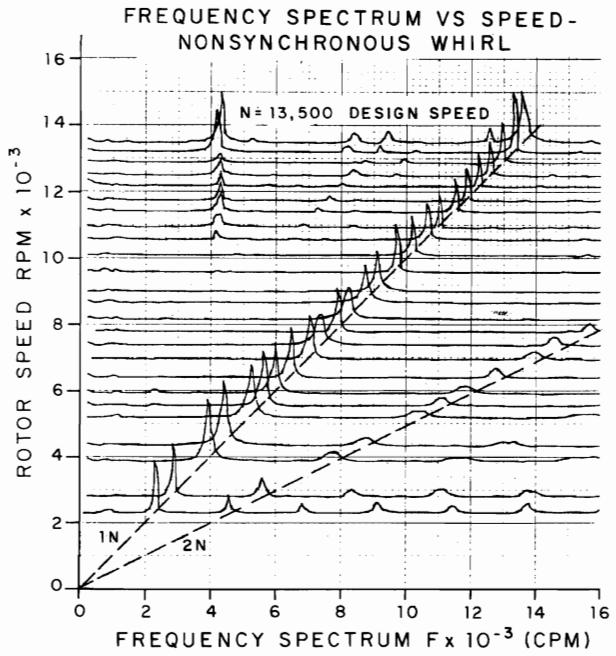

Figure 5-2. Frequency Spectrum vs Speed — Nonsynchronous Whirl.

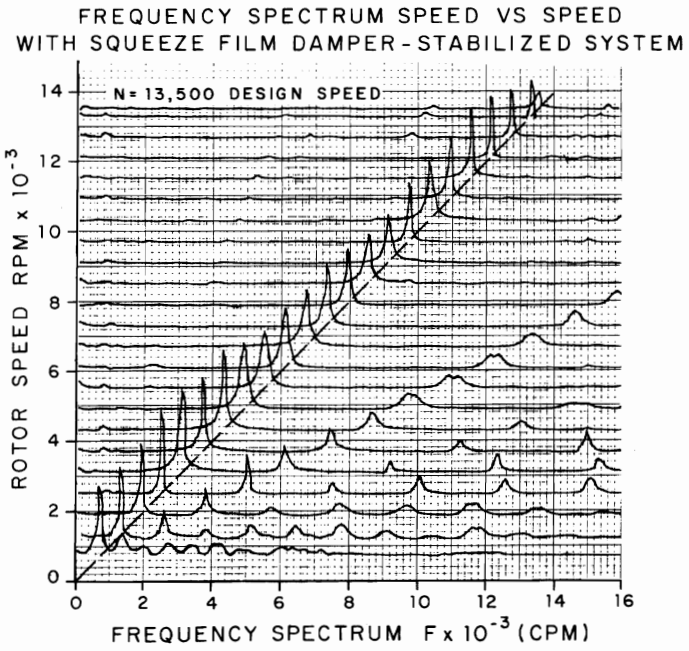

Figure 5-3. Frequency Spectrum Speed vs Speed with Squeeze Film Dampers — Stabilized System.

there is no way that balancing the rotor alone could reduce or remove the self-excited nonsynchronous component in the rotor. It may also be of interest to note that the two times component has not been reduced by the squeeze film dampers or by balancing the rotor. It may well be that the two times component is caused by a misaligned coupling, and that a hot alignment should be performed on the machine.

Oscilloscope traces of the rotor orbits before and after stabilization are shown in Figure 5.4. Figure 5.4a shows that the total motion includes both synchronous and nonsynchronous components of vibration at the operating speed of 13,500 RPM. Following stabilization of the rotor with dampers, Figure 5.4b shows nonsynchronous motion on the upper trace and total motion on the lower trace. The resulting total motion is nearly all synchronous because the nonsynchronous component is very small.

The history of this compressor over a period of years showed slowly increasing vibration levels following each replacement of seals and bearings until wear became excessive. No large vibrations, either synchronous or nonsynchronous, were observed in the rotor operation over an eight month period after the dampers were installed.

CONCLUSIONS

1. Self-excited whirl motion may be created in turbomachinery by one or more of the following effects; aerodynamic cross-coupling internal friction, fluid film bearings and seals, balance pistons, and labyrinths.
2. The use of tilting pad bearings does not guarantee stable operation because of other effects as mentioned above.
3. Long multi-stage turborotors operating at several times the rotor first critical speed may be very susceptible to self-excited whirl instability.

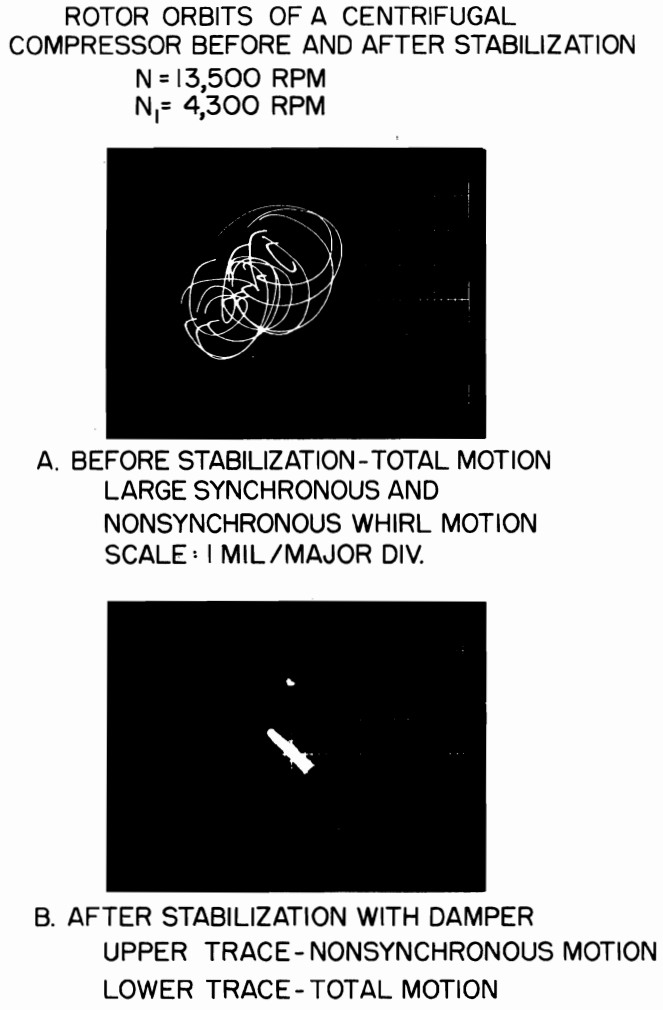

Figure 5-4. Rotor Orbits of a Centrifugal Compressor Before and After Stabilization, N=13,500 RPM, N1=4,300 RPM.

4. With short rigid rotors, stability may be improved by a reduction of clearance of the tilting pad bearings, whereas with long flexible rotors, a reduction of bearing clearance can lead to catastrophic failure.
5. Stability may be improved by the following
   a. Reduction in operating speed or power level
   b. Reduction of instability mechanisms
   c. Increase in effective shaft stiffness
   d. Increase in effective rotor modal damping
6. Properly designed squeeze film dampers can improve stability and unbalance response characteristics of turbomachinery by increasing the modal damping.
7. The damper characteristics must be sized for a particular rotor-bearing system.
8. For a given damper design there is a limit to the level of self-excitation that it can stabilize.
9. The higher the level of aerodynamic cross-coupling the more carefully the damper must be tuned to the rotor.
10. The self excited motion at the center of the rotor may be considerably greater than the motion monitored at or near the bearings.

11. Excessive squeeze film stiffness or damping will reduce the effectiveness of the damper.
12. The squeeze film damper characteristics are highly nonlinear functions of the eccentricity ratio and hence the damper may not function properly under excessive loading.

REFERENCES

1. Kirk, R. G. and E. J. Gunter, "Transient Journal Bearing Analysis," NASA CR-1549, 1970.
2. Apfel, R. E., "The Tensile Strength of Liquids," *Scientific American*, December, 1972, p. 58.
3. White, D. C. "Squeeze Film Journal Bearings," Ph.D. Dissertation, Cambridge University, 1970.
4. Booker, J. F., "A Table of the Journal Bearing Integral," ASME, *Jour. of Basic Engineering*, June, 1965, p. 533.
5. Jeffcott, H. H., "The Lateral Vibrations of Loaded Shafts in the Neighborhood of a Whirling Speed . . . the Effect of Want of Balance," *Phil. Mag.* Series 6, Vol. 37, 1919, p. 304.
6. Newkirk, B. L., "Shaft Whipping," *Gen. Elec. Rev.*, Vol. 27, 1924, p. 169.
7. Kimball, A. L., "Internal Friction as a Cause of Shaft Whirling," *Phil. Mag.*, Vol. 49, 1925, pp. 724-727.
8. Newkirk, B. L. and H. D. Taylor, "Shaft Whipping Due to Oil Action in Journal Bearing," *Gen. Elec. Rev.*, Vol. 28, 1925, pp. 559-568.
9. Robertson, D., "Whirling of a Journal in a Sleeve Bearing," *Phil. Mag.*, Series 7, Vol 15, 1933, pp. 113-130.
10. Poritsky, H., "Contribution to the Theory of Oil Whip," *Trans. ASME*, August 1953, pp. 1153-1161.
11. Pinkus, O., and B. Sternlicht, *Theory of Hydrodynamic Lubrication*, McGraw Hill, New York, 1961.
12. Alford, J. S., "Protecting Turbomachinery From Self-Excited Rotor Whirl," *ASME Jour. of Engr. for Power*, Vol. 87, October 1965, pp. 333-344.
13. Kirk, R. G. and E. J. Gunter, "The Influence of Damper Supports on the Dynamic Response of a Single Mass Flexible Rotor — Part I, Linear Systems," RLES, No. ME-4040-105-71U, March 1971, University of Virginia for NASA Lewis Research Center.
14. Gunter, E. J., "Dynamic Stability of Rotor-Bearing Systems," NASA SP-113, 1966.
15. Choudhury, P. De, "Dynamic Stability of Flexible Rotor-Bearing Systems," Ph.D. Dissertation, University of Virginia, June, 1971.
16. Kirk, R. G. and E. J. Gunter, "SDSTB," Computer program, University of Virginia.
17. Ruhl, R. L., "Dynamics of Distributed Parameter Rotor Systems: Transfer Matrix and Finite Element Techniques," Ph.D. Dissertation, Cornell University, 1970.
18. Bansal, P. N., "Application of Transfer Matrix Method for the Stability Analysis of Multi-Mass Flexible Rotors," University of Virginia Report, unpublished, 1973.
19. Barrett, L. E. and E. J. Gunter, "BRGTRAN," Computer program University of Virginia.
20. Mohan, S. and E. Hahn, "Squeeze Film Bearing Simulation and Design Considerations," RLES Report No. ME-4040-107-720, University of Virginia, June 1972.
21. Kirk, R. G. and E. J. Gunter "TMASSNL," Computer Program, University of Virginia.